

Journal of Organometallic Chemistry, 406 (1991) 399–408

Elsevier Sequoia S.A., Lausanne

JOM 21536

Synthesis and crystal structure of a platinum–silver cluster compound, $[\text{Pt}_3\text{Ag}(\text{O}_3\text{SCF}_3)(\mu\text{-CO})_3(\text{PCy}_3)_2(\text{dppp})]$ ($\text{Cy} = \text{C}_6\text{H}_{11}$, $\text{dppp} = \{(\text{C}_6\text{H}_5)_2\text{P}\}_2\text{C}_3\text{H}_6$) with a distorted tetrahedral geometry

Andrew D. Burrows, John G. Jeffrey, Jonathan C. Machell
and D. Michael P. Mingos *

Inorganic Chemistry Laboratory, University of Oxford, South Parks Road, Oxford OX1 3QR (UK)

(Received September 21st, 1990)

Abstract

The cluster compound $[\text{Pt}_3\text{Ag}(\text{O}_3\text{SCF}_3)(\mu\text{-CO})_3(\text{PCy}_3)_2(\text{dppp})]$ (2) ($\text{Cy} = \text{C}_6\text{H}_{11}$, $\text{dppp} = \{(\text{C}_6\text{H}_5)_2\text{P}\}_2\text{C}_3\text{H}_6$) has been obtained in high yield from the reaction between $[\text{Pt}_3(\mu\text{-CO})_3(\text{PCy}_3)_2(\text{dppp})]$ (1) and $\text{AgCF}_3\text{SO}_3^-$. The molecular structure of $[\text{Pt}_3\text{Ag}(\text{O}_3\text{SCF}_3)(\mu\text{-CO})_3(\text{PCy}_3)_2(\text{dppp})]\cdot 2\text{C}_6\text{H}_5\text{CH}_3$ has been determined by X-ray diffractometry. The structure is based on a distorted tetrahedron. One Pt–Pt bond is significantly shorter, at 2.653(2) Å, than the other two, which have lengths of 2.709(2) and 2.697(2) Å, respectively. Similarly one Pt–Ag bond is, at 2.690(3) Å, considerably shorter than the other two, which are 2.927(3) and 2.919(4) Å. The CF_3SO_3^- anion is coordinated weakly to the silver through one oxygen atom ($\text{Ag}–\text{O} = 2.30(3)$ Å). $^{31}\text{P}\{\text{H}\}$ NMR studies have demonstrated that the tetrahedral structure is maintained in solution.

Introduction

The 42 and 44 electron platinum triangular cluster compounds $[\text{Pt}_3(\mu\text{-CO})_3(\text{PCy}_3)_3]$ and $[\text{Pt}_3(\mu\text{-SO}_2)_2(\mu\text{-X})(\text{PCy}_3)_3]^-$ ($\text{X} = \text{Cl}$, Br or I) are sufficiently nucleophilic to react with MPR_3^+ ($\text{M} = \text{Cu}$, Ag or Au) fragments [1–4]. The former, when reacted with AuPPPh_3^+ , results in the formation of a tetrahedral cluster $[\text{Pt}_3\text{Au}(\mu\text{-CO})_3(\text{PCy}_3)_3(\text{PPh}_3)]^+$, whereas the latter with $\text{Au}\{(\text{P}(p\text{-C}_6\text{H}_4\text{F})_3)\}^+$ can give rise to either tetrahedral $[\text{Pt}_3\text{Au}(\mu\text{-Cl})(\mu\text{-SO}_2)_2(\text{PCy}_3)_3(\text{P}(p\text{-C}_6\text{H}_4\text{F})_3)]$ or trigonal bipyramidal $[\text{Pt}_3\text{Au}_2(\mu\text{-Cl})(\mu\text{-SO}_2)_2(\text{PCy}_3)_3(\text{P}(p\text{-C}_6\text{H}_4\text{F})_3)_2]^+$ clusters. In the latter the gold atoms occupy axial sites of the trigonal bipyramidal. Sandwich cluster compounds where Cu , Ag or Au atoms are coordinated between two $[\text{Pt}_3(\mu\text{-CO})_3(\text{PPh}_3)_3]$ clusters have also been characterised using single crystal X-ray crystallographic techniques [5,6]. Although some years ago we reported the synthesis of an alternative class of 44-electron platinum triangular cluster compounds, $[\text{Pt}_3(\mu\text{-CO})_3(\text{PCy}_3)_2(\text{dppp})]$ and $[\text{Pt}_3(\mu\text{-SO}_2)_3(\text{PCy}_3)_2(\text{dppp})]$ [7], we have not previously reported their reactions with group 11 metal cations, which are isolobal with H^+ .

Since X-ray crystallographic studies indicated that these 44-electron triangular clusters are sterically crowded, their reactions with Ag^+ rather than MPPh_3^+ ($\text{M} = \text{Cu}, \text{Ag}$ or Au) were investigated.

Results and discussion

AgO_3SCF_3 reacts rapidly with $[\text{Pt}_3(\mu\text{-CO})_3(\text{PCy}_3)_2(\text{dppp})]$ (**1**) in benzene giving $[\text{Pt}_3\text{Ag}(\text{O}_3\text{SCF}_3)(\mu\text{-CO})_3(\text{PCy}_3)_2(\text{dppp})]$ (**2**) as a bright red crystalline solid in high yield. The structure of **2** has been confirmed by a single crystal X-ray diffraction study. The relevant details of the crystallographic study are given in Table 1. Selected intramolecular bond lengths and angles are given in Table 2. The structure of the molecule revealed by the crystallographic analysis is illustrated in Fig. 1.

The structural analysis has confirmed the tetrahedral structure based on Ag capping the platinum triangle indicated by spectroscopic data. However, the single crystal structural analysis has demonstrated that the tetrahedron is extremely distorted. The Pt(1)–Pt(2) bond is significantly shorter, at 2.653(2) Å, than the other two platinum–platinum bonds in the triangle which have lengths of 2.709(2) and 2.697(2) Å. Furthermore, the Pt(3)–Ag(1) bond is significantly shorter at 2.690(3) Å than the other two Pt–Ag bonds, which have lengths of 2.927(3) and 2.919(2) Å. The CF_3SO_3^- anion is coordinated to the Ag atom through one oxygen atom, Ag(1)–O(1) = 2.30(3) Å, with a second oxygen atom making a much longer contact, Ag(1)–O(3) = 2.95(4) Å. The Ag(1)–O(1) bond is essentially *trans* to the short Pt(3)–Ag(1) bond. The Pt(3)–Ag(1)–O(1) bond angle is 154.2(8)°, compared with the Pt(1)–Ag(1)–O(1) angle of 129.9(8)°.

The distorted tetrahedral cluster geometry has also been observed for $[\text{Pt}_3\text{Ag}(\mu\text{-CO})_3(\text{PPh}_3)_5]^+$ [8] and $[\text{Pt}_3\text{Au}(\mu\text{-CO})_3(\text{PPh}_3)_5]^+$ [9]. In all these examples the

Table 1

Structural details for $[\text{Pt}_3\text{Ag}(\text{O}_3\text{SCF}_3)(\mu\text{-CO})_3(\text{PCy}_3)_2(\text{dppp})]$

Compound	$\text{C}_{81}\text{H}_{72}\text{AgF}_3\text{P}_4\text{Pt}_3\text{O}_6\text{S}$		
Molecular weight	2047.54		
Space group	$P\bar{2}_1/a$		
Cell dimensions	a	27.22(1) Å	α 90°
	b	14.743(4) Å	β 107.50(2)°
	c	21.312(3) Å	γ 90°
Cell volume		8156 Å ³	
Z		4	
Density		1.67 g/cm ³	
Linear absorption coefficient		55.73 cm ⁻¹	
Radiation	Mo- K_α ($\lambda = 0.71069$ Å)		
Standard reflections	8 – 6 – 1, 6 6 – 2, – 8 1 8		
Decay of standards	12%		
2θ range	0–36°		
Number of parameters varied	378		
R	0.0507		
R_w	0.0579		
Goodness of fit	1.15		
$F(000)$	3960		
Residual electron density	1.23 eÅ ⁻³		

Table 2

Selected bond lengths (Å) and angles (°) for $[\text{Pt}_3\text{Ag}(\text{O}_3\text{SCF}_3)(\mu\text{-CO})_3(\text{PCy}_3)_2(\text{dppp})]$

Pt(1)–Pt(2)	2.653(2)	Pt(1)–Pt(3)	2.709(2)
Pt(1)–Ag(1)	2.927(3)	Pt(1)–Pt(1)	2.27(1)
Pt(1)–C(80)	1.97(4)	Pt(1)–C(82)	1.94(5)
Pt(2)–Pt(3)	2.697(2)	Pt(2)–Ag(1)	2.919(4)
Pt(2)–P(2)	2.29(1)	Pt(2)–C(80)	1.94(4)
Pt(2)–C(81)	2.03(3)	Pt(3)–Ag(1)	2.690(3)
Pt(3)–P(3)	2.302(9)	Pt(3)–P(4)	2.32(1)
Pt(3)–C(81)	2.13(3)	Pt(3)–C(82)	2.21(5)
Ag(1)–O(1)	2.30(3)	Ag(1)–O(2)	4.35(4)
Ag(1)–O(3)	2.95(4)	C(80)–O(10)	1.34(4)
C(81)–O(11)	1.17(3)	C(82)–O(12)	1.16(5)
C(100)–S(1)	1.79(7)	C(100)–F(1)	1.30(7)
C(100)–F(2)	1.30(7)	C(100)–F(3)	1.32(7)
O(1)–S(1)	1.41(3)	O(2)–S(1)	1.47(3)
O(3)–S(1)	1.45(4)		
Pt(3)–Pt(1)–Pt(2)	60.38(5)	Ag(1)–Pt(1)–Pt(2)	62.87(8)
Ag(1)–Pt(1)–Pt(3)	56.85(8)	P(1)–Pt(1)–Pt(2)	148.8(3)
P(1)–Pt(1)–Pt(3)	150.8(3)	P(1)–Pt(1)–Ag(1)	126.7(3)
Pt(3)–Pt(2)–Pt(1)	60.85(5)	Ag(1)–Pt(2)–Pt(1)	63.16(8)
Ag(1)–Pt(2)–Pt(3)	57.06(8)	P(2)–Pt(2)–Pt(1)	146.6(3)
P(2)–Pt(2)–Pt(3)	151.0(3)	P(2)–Pt(2)–Ag(1)	132.8(3)
Pt(2)–Pt(3)–Pt(1)	58.77(5)	Ag(1)–Pt(3)–Pt(1)	65.66(8)
Ag(1)–Pt(3)–Pt(2)	65.64(8)	P(3)–Pt(3)–Pt(1)	133.8(3)
P(3)–Pt(3)–Pt(2)	147.5(3)	P(3)–Pt(3)–Ag(1)	91.3(3)
P(4)–Pt(3)–Pt(1)	105.3(3)	P(4)–Pt(3)–Pt(2)	106.9(2)
P(4)–Pt(3)–Ag(1)	170.2(3)	P(4)–Pt(3)–P(3)	98.0(4)
Pt(2)–Ag(1)–Pt(1)	53.97(7)	Pt(3)–Ag(1)–Pt(1)	57.49(7)
Pt(3)–Ag(1)–Pt(2)	53.30(7)	O(1)–Ag(1)–Pt(1)	129.9(8)
O(1)–Ag(1)–Pt(2)	148.5(8)	O(1)–Ag(1)–Pt(3)	154.2(8)
Pt(2)–C(80)–Pt(1)	85.5(17)	O(10)–C(80)–Pt(1)	135.7(32)
O(10)–C(80)–Pt(2)	138.6(32)	Pt(3)–C(81)–Pt(2)	80.9(13)
O(11)–C(81)–Pt(2)	138.5(28)	O(11)–C(81)–Pt(3)	140.5(28)
Pt(3)–C(82)–Pt(1)	81.2(18)	O(12)–C(82)–Pt(1)	150.7(40)
O(12)–C(82)–Pt(3)	128.0(37)	F(1)–C(100)–S(1)	115.8(55)
F(2)–C(100)–S(1)	105.4(53)	F(2)–C(100)–F(1)	108.3(64)
F(3)–C(100)–S(1)	107.9(51)	F(3)–C(100)–F(1)	110.2(63)
F(3)–C(100)–F(2)	109.0(64)	S(1)–O(1)–Ag(1)	113.6(19)
O(1)–S(1)–C(100)	107.1(30)	O(2)–S(1)–C(100)	105.1(30)
O(2)–S(1)–O(1)	113.1(22)	O(3)–S(1)–C(100)	102.3(31)
O(3)–S(1)–O(1)	110.9(23)		

shorter Pt–Ag or Pt–Au bond is associated with the more sterically crowded platinum atom. In $[\text{Pt}_3\text{Ag}(\mu\text{-CO})_3(\text{PPh}_3)_5]^+$ the short Pt–Ag distance is 2.741(1) Å c.f. 2.823(1) and 2.915 Å for the longer Pt–Ag distances and in $[\text{Pt}_3\text{Au}(\mu\text{-CO})_3(\text{PPh}_3)_5]^+$ the short Pt–Au distance is 2.700(1) Å c.f. 2.902(2) and 2.910(1) Å for the longer Pt–Au distances.

The $^{31}\text{P}\{\text{H}\}$ NMR spectrum of **2** shows three resonances at 63.0, 33.6 and 6.0 ppm with respect to trimethylphosphate. The corresponding data for the parent triangular cluster (**1**) at room temperature show just two resonances of equal intensity corresponding to the monodendate and bidendate phosphines. The in-

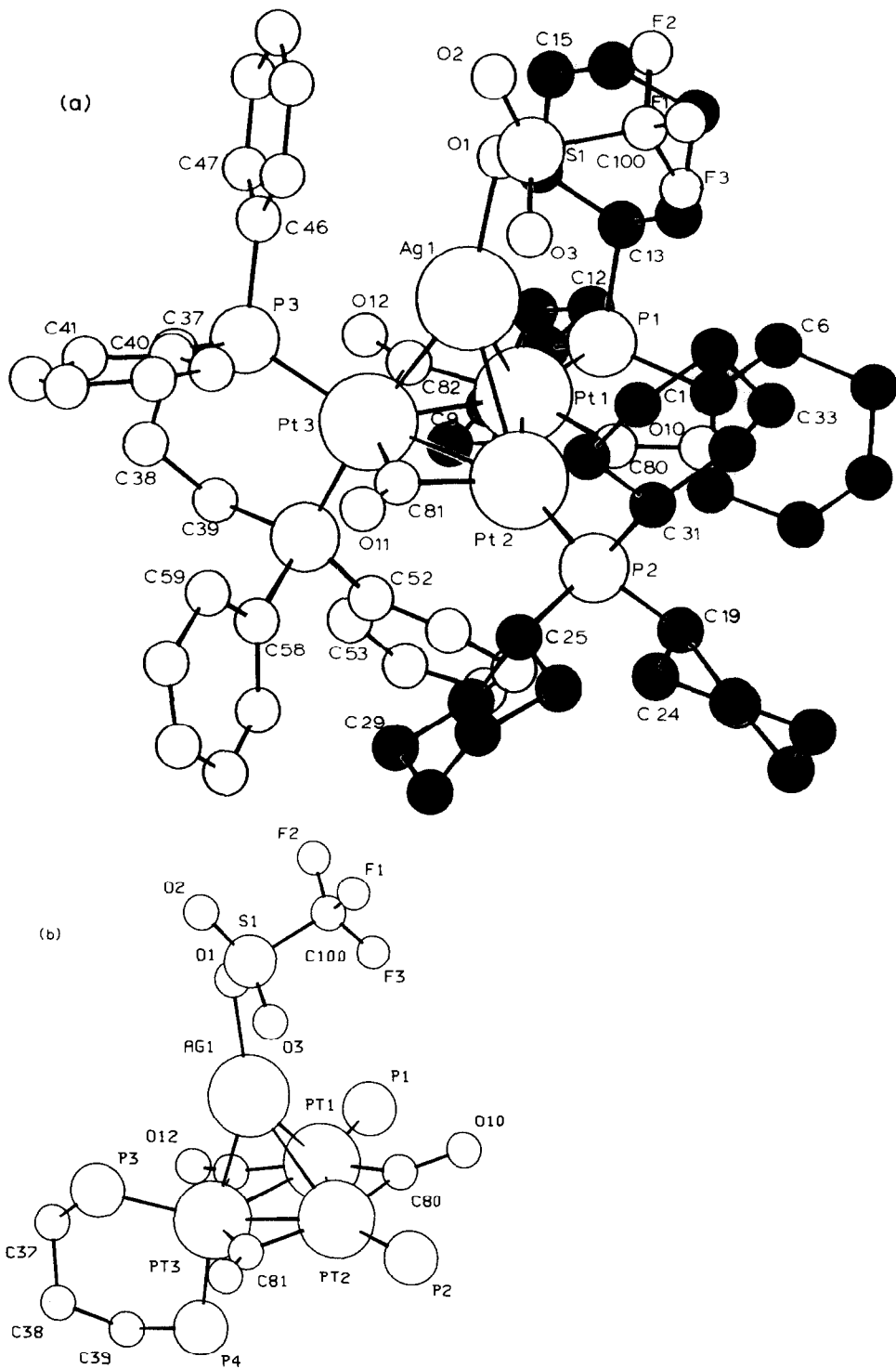


Fig. 1. Molecular structure of $[\text{Pt}_3\text{Ag}(\text{O}_3\text{SCF}_3)(\mu\text{-CO})_3(\text{PCy}_3)_2(\text{dppp})]$ (a) showing all non-hydrogen atoms, the atoms of the cyclohexyl rings are blackered for clarity; (b) with the phenyl and cyclohexyl carbon atoms omitted for clarity.

Table 3 $^{31}\text{P}\{\text{H}\}$ NMR data for $[\text{Pt}_3\text{Ag}(\text{O}_3\text{SCF}_3)(\mu\text{-CO})_3(\text{PCy}_3)_2(\text{dppp})]$ ^a

Chemical shifts	$\delta[\text{P}(1), \text{P}(2)]$	63.0 ppm					
	$\delta[\text{P}(3)]$	33.6 ppm					
	$\delta[\text{P}(4)]$	6.0 ppm					
Coupling constants (Hz)							
	P(2)	P(3)	P(4)	Ag(1)	Pt(1)	Pt(2)	Pt(3)
P(1)	51	51	6	26	4691	283	391
P(2)		51	6	26	283	4691	391
P(3)			22	30	393	393	3578
P(4)				192	88	88	2940

^a This interpretation assumes that the difference in coupling between ^{31}P and ^{107}Ag ($I = 1/2$, 51.8%), and ^{31}P and ^{109}Ag ($I = 1/2$, 48.2%) is not resolved. An alternate interpretation would be to assign $^3J[\text{P}(1) - \text{P}(4)] = 0$ Hz, which would give $^2J[\text{P}(1) - ^{107}\text{Ag}] = 32$ Hz and $^2J[\text{P}(1) - ^{109}\text{Ag}] = 20$ Hz, or vice versa.

equivalence of the phosphorus resonances associated with the dppp ligand in **2** can be attributed to the coordination of Ag^+ to one face of the triangular cluster. The $^{31}\text{P}\{\text{H}\}$ NMR spectrum has been satisfactorily simulated using a computer analysis based on a system comprising the isotopomers A_2BCM (no ^{195}Pt nuclei, 29.1%

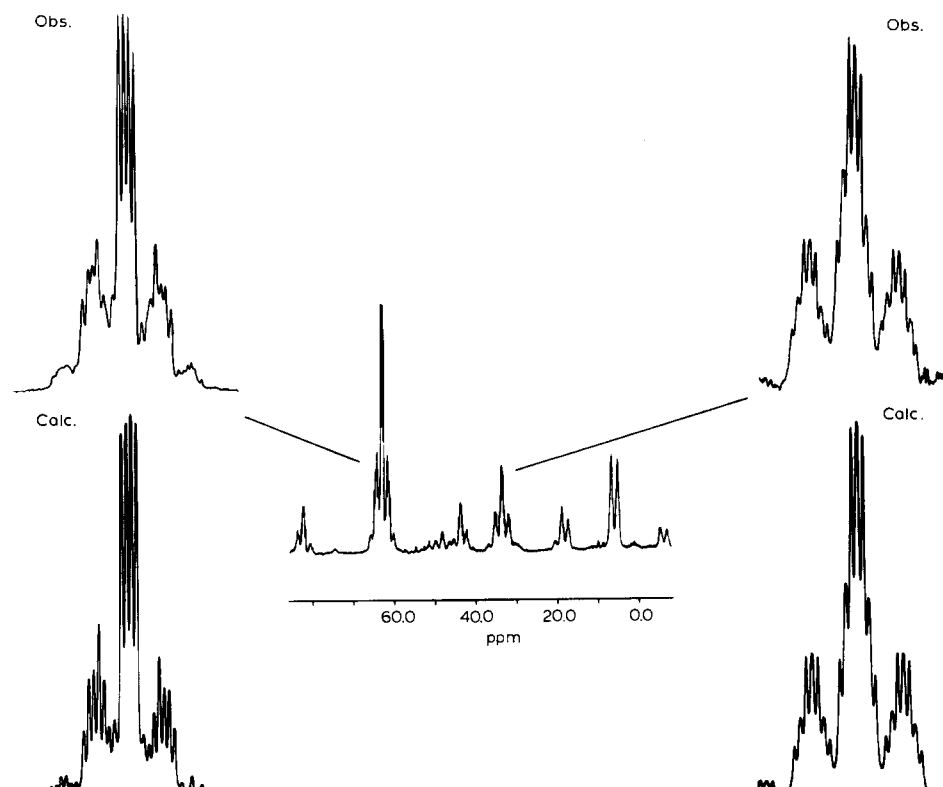


Fig. 2. $^{31}\text{P}\{\text{H}\}$ NMR spectrum of **2**. Expanded views are shown together with the calculated spectrum for the multiplets at 63.0 and 33.6 ppm.

abundance), AA'BCMX (one ^{195}Pt nucleus, X, 29.6% abundance), A_2BCMY (one ^{195}Pt nucleus, Y, 14.8% abundance), AA'BCMXY (two ^{195}Pt nuclei, X and Y, 15.1% abundance), AA'BCMXX' (two ^{195}Pt nuclei, X and X', 7.5% abundance) and AA'BCMXX'Y (three ^{195}Pt nuclei, X, X' and Y, 3.8% abundance). The coupling constants are given in Table 3 and the relevant spectra are illustrated in Fig. 2. The resonances show rather different line widths, which do not become sharper on cooling to -40°C , and could be associated with asymmetric relaxation effects for the different phosphorus environments.

The P–P and P–Pt coupling constants for **2** show differences from those associated with **1** which can be understood in terms of the distortion of the PtL_2 fragment, which itself is a consequence of the capping atom. This distortion breaks the symmetry of the dppp ligand, and leads to the Pt(3)–P(3) bond becoming closer to the plane of the Pt_3 triangle, and the Pt(3)–P(4) bond becoming nearer the perpendicular. This results in the coupling constants for P(3) with P(1) and P(2), and with Pt(1) and Pt(2), becoming larger with respect to **1**: $^3J[\text{P}(1)\text{–P}(3)] = 51\text{ Hz}$ (19 Hz for **1**) and $^2J[\text{Pt}(1)\text{–P}(3)] = 393\text{ Hz}$ (270 Hz), whereas those for P(4) are decreased: $^3J[\text{P}(1)\text{–P}(4)] = 6\text{ Hz}$ (19 Hz) and $^2J[\text{Pt}(1)\text{–P}(4)] = 88\text{ Hz}$ (270 Hz).

The geometry of the Pt_3AgP_4 core in **2** also influences the $^2J[\text{Ag–P}]$ coupling constants. The Ag(1)–Pt(3)–P(4) bond angle is $170.2(3)^\circ$ leading to $J[\text{Ag}(1)\text{–P}(4)] = 192\text{ Hz}$, whereas the Ag(1)–Pt(3)–P(3) angle is $91.3(3)^\circ$ with the corresponding coupling constant $J[\text{Ag}(1)\text{–P}(3)] = 30\text{ Hz}$.

The IR spectrum of **2** shows the presence of bridging carbonyl ligands (1861w, 1816m, 1782s cm^{-1}). These signals are all shifted to about 20 cm^{-1} higher in frequency than in **1** (1842w, 1790s, 1763s cm^{-1}). This increase in frequency results from a decrease in the π -back donation consistent with the electroneutrality principle.

Recently molecular orbital calculations have been completed on $[\text{Pt}_3(\mu\text{-CO})_3\text{L}_4]$ ($\text{L} = \text{PH}_3$) clusters [10] which shed some light on the observation that the capping atom bonds more strongly to the more sterically crowded platinum atom. The

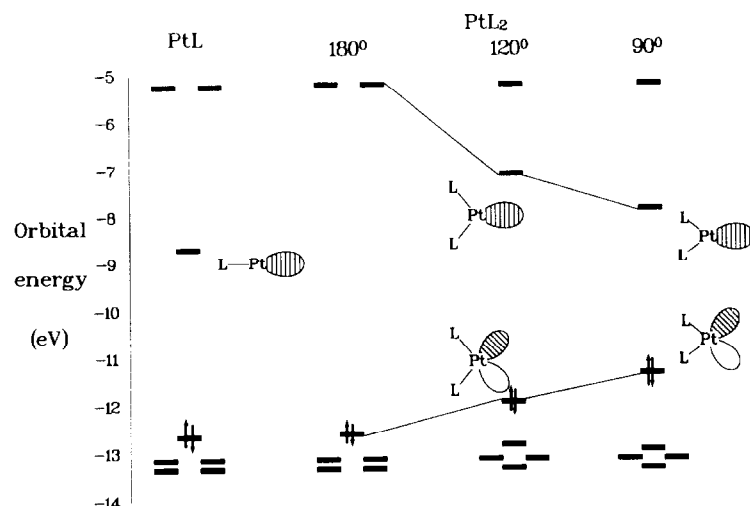


Fig. 3. Frontier orbitals of PtL and PtL_2 as a function of bending angle.

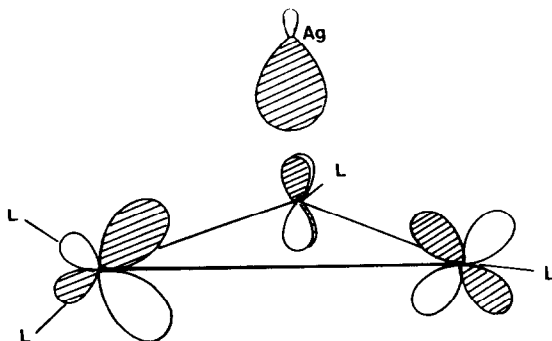


Fig. 4. Important orbital interactions between frontier orbitals on Pt_3L_4 and the Ag^+ sp hybrid.

replacement of a Pt–L fragment in $[\text{Pt}_3(\mu\text{-CO})_3\text{L}_3]$ by an angular PtL_2 fragment to form $[\text{Pt}_3(\mu\text{-CO})_3\text{L}_4]$ can be interpreted in terms of differences in the electronic characteristics of the fragments (see Fig. 3). The PtL_2 fragment has a higher lying HOMO and a lower lying LUMO. The former contributes significantly to a high lying orbital in the $[\text{Pt}_3(\mu\text{-CO})_3\text{L}_4]$ cluster of b_1 symmetry which is illustrated schematically in Fig. 4. The higher localisation of the platinum dp hybrid on the PtL_2 fragment and its hybrid character ensures that the overlap with the outpointing sp hybrid of the AgL fragment is larger for the more sterically crowded platinum. Therefore, the shorter Ag–Pt bonds to this atom can be directly related to the higher nucleophilicity of this atom.

These molecular orbital calculations have indicated that the Pt–Pt bond opposite the PtL_2 fragment should be shorter than the other two Pt–Pt bonds. This is borne out by the present structural analyses, where it has been established that this bond is ca. 0.05 Å shorter than the other Pt–Pt bonds.

Experimental

Reactions were routinely carried out, using standard Schlenk-line procedures, under an atmosphere of pure, dry dinitrogen and using dry, deoxygenated solvents. Microanalyses were carried out by Mr. M. Gasgoyne and his staff of this laboratory. Infrared spectra were recorded as Nujol mulls using a Perkin–Elmer 1710 FT-spectrometer.

$^{31}\text{P}\{^1\text{H}\}$ NMR spectra were recorded using a Bruker AM-300 spectrometer operating at 121.51 MHz referenced to trimethoxyphosphate. NMR computer simulations were carried out using the Oxford University VAX computer system using a program developed by Prof. R.K. Harris, then of the University of East Anglia, and adapted for use at Oxford by Dr. A.E. Derome. $[\text{Pt}_3(\mu\text{-CO})_3(\text{PCy}_3)_3]$ was synthesised by the method of Clark et al. [11] from *trans*- $[\text{PtH}_2(\text{PCy}_3)_2]$ and CO. $[\text{Pt}_3(\mu\text{-CO})_3(\text{PCy}_3)_2(\text{dPPP})]$ was synthesised from the reaction of $[\text{Pt}_3(\mu\text{-CO})_3(\text{PCy}_3)_3]$ and dPPP [7].

Synthesis of $[\text{Pt}_3\text{Ag}(\text{O}_3\text{SCF}_3)(\mu\text{-CO})_3(\text{PCy}_3)_2(\text{dPPP})] \cdot 2\text{C}_6\text{H}_6$ (2)

A solution of $\text{AgCF}_3\text{SO}_3 \cdot 1/2\text{C}_6\text{H}_6$ (0.051 g, 0.17 mmol) in benzene (10 cm³) was added to a solution of $[\text{Pt}_3(\mu\text{-CO})_3(\text{PCy}_3)_2(\text{dPPP})]$ (0.280 g, 0.17 mmol) in benzene (30 cm³). The mixture was stirred for 60 min in darkness. The volume of solvent was

Table 4

Atom coordinates

Atom	<i>x</i>	<i>y</i>	<i>z</i>	<i>U</i> _{iso}
Pt(1)	1611.3(5)	2558(1)	1945.1(7)	391
Pt(2)	824.8(6)	1801(1)	2241.1(7)	397
Pt(3)	1644.3(5)	2381(1)	3222.4(7)	391
Ag(1)	1804(1)	828(2)	2650(2)	613
P(1)	1966(4)	3039(7)	1164(5)	503
P(2)	-15(4)	1327(7)	1862(5)	527
P(3)	2287(4)	2029(7)	4173(5)	508
P(4)	1434(4)	3801(7)	3533(5)	467
C(1)	1492(14)	3190(26)	317(17)	636(116)
C(2)	1068(15)	3873(26)	299(20)	713(128)
C(3)	646(16)	3733(28)	-330(21)	816(140)
C(4)	835(19)	3732(34)	-913(25)	1152(185)
C(5)	1236(15)	3112(27)	-919(19)	723(123)
C(6)	1715(14)	3261(27)	-260(18)	694(121)
C(7)	2347(12)	4084(21)	1376(15)	384(97)
C(8)	2632(13)	4416(24)	904(17)	514(113)
C(9)	2965(13)	5236(24)	1170(18)	582(114)
C(10)	2662(15)	6006(27)	1457(20)	747(131)
C(11)	2370(19)	5678(34)	1882(24)	1103(174)
C(12)	2012(14)	4817(25)	1562(18)	629(120)
C(13)	2433(12)	2181(21)	1067(16)	418(100)
C(14)	2864(14)	2000(25)	1688(18)	603(114)
C(15)	3258(16)	1309(29)	1639(20)	826(144)
C(16)	2943(17)	432(29)	1347(22)	859(143)
C(17)	2532(18)	548(32)	716(24)	1031(169)
C(18)	2126(15)	1303(26)	804(19)	692(128)
C(19)	-371(14)	1969(26)	1115(18)	627(121)
C(20)	-992(17)	1717(31)	842(21)	945(148)
C(21)	-1180(15)	2173(28)	155(20)	782(136)
C(22)	-1081(18)	3185(33)	143(22)	1039(161)
C(23)	-512(18)	3387(32)	440(24)	1080(167)
C(24)	-295(15)	3035(29)	1128(20)	767(135)
C(25)	-332(13)	1333(23)	2521(17)	488(106)
C(26)	-863(15)	890(26)	2371(19)	745(128)
C(27)	-993(15)	954(28)	3035(19)	733(131)
C(28)	-1010(14)	1881(27)	3272(18)	644(117)
C(29)	-514(18)	2357(34)	3383(22)	1101(163)
C(30)	-366(12)	2297(24)	2756(16)	493(103)
C(31)	-86(13)	106(24)	1606(17)	554(113)
C(32)	102(16)	-32(29)	948(20)	821(141)
C(33)	14(17)	-1028(32)	822(22)	940(152)
C(34)	273(17)	-1676(31)	1339(23)	992(153)
C(35)	104(15)	-1491(26)	1962(19)	704(123)
C(36)	162(14)	-474(26)	2189(19)	668(122)
C(37)	2639(15)	3009(26)	4514(19)	680(124)
C(38)	2322(15)	3830(27)	4663(20)	706(129)
C(39)	2005(15)	4378(27)	4066(20)	763(135)
C(40)	2144(13)	1511(24)	4876(17)	500(108)
C(41)	2358(15)	1788(28)	5491(21)	756(126)
C(42)	2210(15)	1438(27)	6007(19)	651(121)
C(43)	1878(18)	724(33)	5904(24)	1003(159)
C(44)	1668(14)	358(24)	5300(18)	564(113)
C(45)	1763(13)	783(24)	4744(16)	473(105)

Table 4 (continued)

Atom coordinates

Atom	<i>x</i>	<i>y</i>	<i>z</i>	<i>U</i> _{iso}
C(46)	2805(16)	1262(34)	4099(19)	1669(111)
C(47)	3288(22)	1700(21)	4053(19)	1669(111)
C(48)	3698(14)	1133(37)	4000(18)	1669(111)
C(49)	3627(16)	127(33)	3991(18)	1669(111)
C(50)	3145(22)	– 311(21)	4037(19)	1669(111)
C(51)	2734(15)	256(37)	4091(19)	1669(111)
C(52)	1190(13)	4641(25)	2897(17)	471(107)
C(53)	1358(17)	5527(32)	2890(22)	879(149)
C(54)	1146(17)	6098(28)	2387(23)	826(140)
C(55)	772(15)	5838(28)	1856(19)	648(123)
C(56)	594(16)	4988(29)	1788(20)	715(130)
C(57)	797(18)	4481(30)	2369(25)	940(152)
C(58)	965(13)	3748(25)	4015(18)	496(109)
C(59)	1031(15)	3120(28)	4506(20)	749(129)
C(60)	663(16)	3158(30)	4901(19)	800(134)
C(61)	325(21)	3854(38)	4745(27)	1194(188)
C(62)	270(20)	4494(37)	4267(28)	1224(192)
C(63)	626(20)	4516(35)	3934(24)	1110(177)
C(80)	956(16)	2034(28)	1408(21)	822(144)
C(81)	970(13)	1653(23)	3226(17)	436(99)
C(82)	2153(19)	2997(31)	2702(23)	1004(165)
C(100)	1867(31)	– 1556(52)	1603(37)	1756(284)
C(200)	1262(18)	3851(33)	7299(20)	1805(115)
C(201)	742(24)	4129(23)	7267(22)	1805(115)
C(202)	318(14)	3488(40)	7052(22)	1805(115)
C(203)	415(18)	2569(34)	6869(18)	1805(115)
C(204)	935(24)	2292(23)	6901(19)	1805(115)
C(205)	1358(14)	2933(40)	7117(21)	1805(115)
C(300)	4287(18)	2607(32)	5376(18)	1685(112)
C(301)	4506(14)	3470(41)	5400(20)	1685(112)
C(302)	4403(17)	4140(23)	5809(25)	1685(112)
C(303)	4081(18)	3946(32)	6193(19)	1685(112)
C(304)	3861(13)	3083(41)	6168(20)	1685(112)
C(305)	3964(16)	2414(24)	5760(25)	1685(112)
O(1)	2286(12)	– 397(22)	2516(15)	1136(111)
O(2)	2335(14)	– 1971(24)	2818(18)	1470(138)
O(3)	1514(16)	– 1104(26)	2527(20)	1634(152)
O(10)	739(10)	1857(18)	769(12)	800(86)
O(11)	769(9)	1352(16)	3593(12)	596(75)
O(12)	2532(10)	3392(19)	2925(13)	792(88)
S(1)	2019(6)	– 1228(10)	2448(7)	1022(45)
F(1)	1606(12)	– 2307(24)	1443(16)	1552(120)
F(2)	2311(15)	– 1660(25)	1495(18)	1817(142)
F(3)	1617(12)	– 877(23)	1238(16)	1506(121)

reduced *in vacuo* and hexane added to give a red solid. Recrystallisation from benzene/hexane gave 0.237 g (73%) of product as dark red crystals. (Found: C, 45.9; H, 5.0. C₇₉H₁₀₄AgF₃O₆P₄Pt₃S calc.: C, 46.1; H, 5.1%); ν (CO) at 1861w, 1816m, 1782s cm⁻¹.

Crystal data for $C_{67}H_{92}AgF_3O_6P_4Pt_3S \cdot 2C_6H_5CH_3$

Red crystals were grown by the slow diffusion of hexane into a toluene solution of **2**. A single crystal of dimensions $0.5 \times 0.5 \times 0.5$ mm was mounted in a glass capillary. Diffraction data were collected on a CAD4 diffractometer. 6738 reflections were collected by $\omega/2\theta$ scans (scan width $0.70 + 0.35 \tan \theta$), of which 2741 were considered unique and observed ($I \geq 3\sigma(I)$, $R_{\text{merg}} = 0.0423$). These were corrected for Lorentz and polarisation effects and an empirical absorption correction was applied (min/max correction 1.00/2.51).

The structure was solved by a combination of Patterson and the TRIAL instruction in CRYSTALS, and Fourier methods, and full-matrix least-squares refinement of all the non-hydrogen atoms. One of the phenyl groups on the dppp ligand was refined as a rigid group. After converting the platinum, silver and phosphorus atoms to have anisotropic thermal parameters, the hydrogen atoms were generated geometrically. On application of a Chebyshev weighting scheme (coefficients 4.881, -4.975, 3.715, -1.245), the model converged at $R = 0.0507$, $R_w = 0.0579$. Programs and sources of scattering factor data are given in the references [12,13]. The atom coordinates are shown in Table 4. Lists of structure factors are available from the authors.

References

- 1 C.E. Briant, R.W.M. Wardle and D.M.P. Mingos, *J. Organomet. Chem.*, 267 (1984) C49.
- 2 D.M.P. Mingos and R.W.M. Wardle, *J. Chem. Soc., Dalton Trans.*, (1986) 73.
- 3 D.M.P. Mingos, P. Oster and D.J. Sherman, *J. Organomet. Chem.*, 320 (1987) 257.
- 4 P. Braunstein, S. Freyburger and O. Bars, *J. Organomet. Chem.*, 352 (1988) C29.
- 5 A. Albinati, K.-H. Dahmen, A. Togni and L.M. Venanzi, *Angew. Chem., Int. Ed. Engl.*, 24 (1985) 766.
- 6 M.F. Hallam, D.M.P. Mingos, T. Adatia and M. McPartlin, *J. Chem. Soc., Dalton Trans.*, (1988) 335.
- 7 M.F. Hallam, N.D. Howells, D.M.P. Mingos and R.W.M. Wardle, *J. Chem. Soc., Dalton Trans.*, (1985) 845.
- 8 S. Bhaduri, K. Sharma, P.G. Jones and C. Erdbrugger, *J. Organomet. Chem.*, 326 (1987) C46.
- 9 J.J. Bour, R.P.F. Kanders, P.P.J. Schlebos, W. Bos, W.P. Bosman, H. Behm, P.T. Beurskens and J.J. Steggerda, *J. Organomet. Chem.*, 329 (1987) 405.
- 10 D.M.P. Mingos and T. Slee, *J. Organomet. Chem.*, 394 (1990) 679.
- 11 H.C. Clark, A.B. Goel and C.S. Wong, *Inorg. Chim. Acta*, 34 (1979) 159.
- 12 D.J. Watkin, J.R. Carruthers and P.W. Ritteridge, *CRYSTALS User Manual*, Chemical Crystallography Laboratory, University of Oxford, 1985.
- 13 International Tables of Crystallography, Kynoch Press, Birmingham, 1974.